CFD Modeling Study of High Temperature and Low Oxygen Content Exhaust Gases Combustion Furnaces

Abbasi Khazaei, Kiomars*+

Graduate School of the Environment and Energy, Science and Research Branch, Islamic Azad University, P.O. Box 14155-4933 Tehran, I.R. IRAN

Hamidi, Ali Asghar

Faculty of Chemical Engineering, Tehran University, P.O. Box 11155-4563 Tehran, I.R. IRAN

Rahimi, Masoud

CFD Research Center, Department of Chemical Engineering, Razi University, Kermanshah, I.R. IRAN

ABSTRACT: *This paper reports a CFD modeling study on the possibility of using high temperature and low oxygen content exhaust gases as oxidant for combustion in an industrial furnace by a written computer program. Under these conditions, the predicted results for the flow and heat transfer properties are compared with those under the several cases of conventional and highly preheated and diluted air combustion (HPDAC) conditions. Although the calculation procedure is a two dimensional one with the vorticity and stream function as the main hydrodynamic variables; its results can yet be also valid for the three dimensional case. Because of the weakness of the standard or other traditional k-ε models in predicting the spreading rate of axisymmetric jets, and also for the sake of economy and lack of boundary conditions, here the turbulent transport properties are obtained from an algebraic formula. An infinitely single-step chemical reaction (physically controlled) and a model known as "four flux" are considered as combustion and radiation models, respectively. The qualitative and quantitative verification of high temperature and low oxygen content air/exhaust gases combustions and conventional (low and high air temperature) combustions results have been checked and compared , respectively, with those reported in the literature. Finally, in this investigation three modified concepts and new formulas have been proposed and used to define the gas temperature uniformity, the chemical flame size and the maximum flame temperature as the HPDAC'S main unique features achievement criteria.*

KEY WORDS: *HPDAC, CFD modeling, Low oxygen content exhaust gases, Energy saving, Thermal-NO.*

* *To whom correspondence should be addressed.*
+ *E-mail: kns_abbasi@yahoo.com*
1021-9986/10/2/85 20/$/4.00

INTRODUCTION

High energy saving along with the low pollutant emissions are the world's energy-environmental main requirements. These requirements can be complied with the one of the most promising combustion techniques, i.e., the highly preheated and diluted air combustion (HPDAC). The HPDAC applied to industrial furnaces offers simultaneous main unique features such as: high energy savings, more uniform and relatively moderate gas temperature profile and thus a reduction in pollutant emissions, a larger flame and thus a low maximum local heat release rate as well as the possibility of low combustion noise, and high quality of product at increased production rate [1-3].

This technology which is based on very efficient preheating of the air/oxidizer by means of a highly efficient heat exchanger in the form of regenerator, was developed more than 10 years back and has been commercially applied in different types of furnaces as reported by *Yasuda & Ueno* [2]. But nevertheless besides experimental works, numerical modeling has also received attention during these years for better explanation of the basic chemical-physical phenomenon. For obtaining adequate knowledge of the features of HPDAC, for instance, *Ishii* [4] and *Shimada* [5] conducted mathematical modeling applied industrial codes FLUENT and STAR-CD respectively to simulate the large scale industrial testing furnaces, in which the standard k-ε model and the probability density function (PDF) model were used to deal with the turbulence-reaction flows and with emphasis on NO_x formation. *Kobayashi* [6] carried out a numerical simulation of two high temperature air combustion boilers with different burner arrangements and emphasis on the capability of HPDAC technology for applying of fuels with high and low calorific values. *Dong* [7] conducted a simulation for the phenomena of turbulent combustion, with an emphasis on jet flames under HPDAC conditions. He used different models such as the finite-rate/eddy-dissipation model (FRED), the mixture fraction/PDF model (MPDF), the standard k-ε model, RNG k-ε model, Reynolds stress model (RSM), Rosseland model and discrete transfer radiation model were used. Numerical simulation of a LPG flame with high-temperature air was carried out by *Yang* [8]. Attention was focused on both the size and shape of the flame.

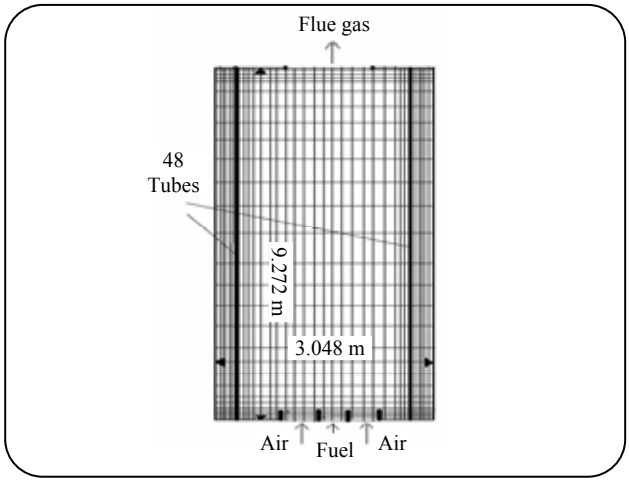

Fig.1: Furnace grid arrangement.

The attentions of the above mentioned valuable numerical studies have been mostly focused on the flame and combustion characteristics under the HPDAC. However in the present work, the investigations have been more intense on calculation of the flow and heat transfer properties under high temperature and low oxygen content exhaust gases (as oxidant) combustion using a different written computer program.

The computational fluid dynamic(CFD) modeling study of this work focused on the HPDAC burning system for a furnace setup presented in Fig. 1; since analyzing the literature on the subject, showed that the study of a single type burner and fuel jet allowed explaining and measuring many unique features of the HPDAC. For example experimental studies were performed by *Blasiak et al*. [9-11] and other researchers.

It is possible to list the main objective of the present work as follow:

- The application of a computer program written by authors including the specific turbulence, combustion and radiation models as well as the three proposed modified concepts and new formulae, for numerical comparative studying of the flow pattern, and also the main unique features, specifically the comparative studying of heat transfer characteristics of furnaces with the high temperature and low oxygen content exhaust gases, HPDAC and conventional combustions.

In this investigation several conditions for the combustion of natural gas fuel are considered:

- Using the low oxygen content exhaust gases (10% O_2) at 1273 K

- Using the diluted air (90% N_2 and 10% O_2) at 1273 K,
- Using the undiluted air (21% O_2) and its ambient temperature/1273 K as oxidants.

In summary, the energy saving, the gas temperature profiles and uniformity and thus the pollutant emissions, the flame size and thus the local heat release rate, the temperature profiles of tubes wall and process fluids and thus the thermal performance of the regenerator and furnace have been investigated through: 1) the net effects of the fuel/oxidant injection momentum flux ratio which is less than one, by maintaining the temperature and oxygen concentration of oxidant; 2) the net effects of the temperature and oxygen concentration[12] for the above mentioned oxidants by maintaining the momentum flux ratio and fuel to oxidant velocity ratio with values which are less than one via varying the fuel and oxidant inlets sizes. As it will be seen later, by adjusting the operating fuel and thus the oxidant flow rates along with varying the size of their inlets, it is possible to optimize the performance of an existing furnace which is a candidate for revamping from a conventional combustion to an high temperature and low oxygen content exhaust gases / HPDAC combustion process.

Besides the above mentioned items, it is possible to say that, using this software the effects of change of burner to tubes distance, the furnace dimension and other such parameters can be easily studied.

MATHEMATICAL MODELING

Mathematical Main Models

The geometry of the furnace arrangements, shown in Fig.1, is encountered in flows with substantial regions of recirculation. The equation used to represent conservation of the flow properties were, therefore, elliptic in form and were expressed in cylindrical coordinates. The general form of the equation is [13]:

$$a_\varphi\left\{\frac{\partial}{\partial Z}\left(\varphi\frac{\partial\psi}{\partial r}\right)-\frac{\partial}{\partial r}\left(\varphi\frac{\partial\psi}{\partial Z}\right)\right\}- \quad (1)$$

$$\frac{\partial}{\partial Z}\left\{b_\varphi r\left(\varphi\frac{\partial\left(c_\varphi\varphi\right)}{\partial Z}\right)\right\}-\frac{\partial}{\partial r}\left\{b_\varphi r\left(\varphi\frac{\partial\left(c_\varphi\varphi\right)}{\partial r}\right)\right\}+rd_\varphi=0$$

With the corresponding values of φ, a_φ, b_φ, c_φ and d_φ indicated in Table 1.

In addition, the equation presented in Table 1, are derived from the formulation of the conservation of mass, momentum, chemical species and energy. The equations for the physical processes such as turbulent transport and radiation are also added to the systems of equations. The need to introduce additional physical model consequently arises because many of the processes that occur in the furnace are far too complex to be handled at fundamental level of calculation.

Conservation equations

It is assumed that 1) no external body forces act on the system 2) species diffusion follows Flick's law 3) the Lewis number for each chemical species is unity 4) the kinetic heating terms in the energy equation are negligible and 5) the gas follows the ideal gas equation of state. With these assumptions, the equations for conservation of mass, momentum, chemical species, and energy may be written as illustrated in Table 1. The instantaneous equations are transformed to yield equations for the time-averaged variables using a procedure known as Reynolds decomposition [14]. It should be noted that by application of the vorticity and stream function as the main hydrodynamic variables instead of velocity components, the pressure term is removed from the equations.

Mathematical Sub Models

Turbulence models

In the momentum, chemical species and energy conservation equations; turbulent transport of momentum, mass and energy may be modeled using the Boussinesq approximation to relate the turbulent fluxes to the mean flow property gradients via turbulent fluxes, based on Newton, Fick and Fourier laws. Since the transport of species, enthalpy, and momentum occur by similar turbulent exchange processes, the turbulent exchange coefficients for species and enthalpy can be assumed proportional to the turbulent viscosity. In summary the main objective of the present model is to evaluate the transport property by calculating the transport viscosity and this will be achieved by using of a "two equations" or "k-ε" model [15]. Here, for the sake of economy and the lack of sufficient boundary conditions and also the weakness of this model for prediction of the spreading rate for axisymmetric jets [16], another formula is used [17] as:

$$\mu_{eff}=k'\cdot D^{2/3}\cdot W^{-1/3}\cdot\rho^{2/3}\cdot\left(m_F^\circ\cdot V_F^2+m_0^\circ\cdot V_0^2\right)^{1/3} \quad (2)$$

Table 1: Conservation equations correspond to Eq. (1).

φ	a_φ	b_φ	c_φ	d_φ
ψ	0	$\frac{1}{\rho r^2}$	1	$-\frac{\omega}{r}$
ω/r	r^2	r^2	μ_{eff}	$-\frac{\partial}{\partial Z}\left(\rho V_3^2\right)-r\left[\frac{\partial}{\partial Z}\left(\frac{V_1^2+V_2^2}{2}\right)\frac{\partial \rho}{\partial r}-\frac{\partial}{\partial r}\left(\frac{V_1^2+V_2^2}{2}\right)\frac{\partial \rho}{\partial Z}\right]$
rV_3	1	$\mu_{eff}\, r^2$	$1/r^2$	0
h	1	$\frac{\mu_{eff}}{\sigma_{h,eff}}$	1	$-S_R$
m_{fu}	1	$\frac{\mu_{eff}}{\sigma_{fu,eff}}$	1	$-R_{fu}$
f	1	$\frac{\mu_{eff}}{\sigma_{f,eff}}$	1	0
K	1	$\frac{\mu_{eff}}{\sigma_{K,eff}}$	1	$-(S_K-\rho\varepsilon)$
ε	1	$\frac{\mu_{eff}}{\sigma_{\varepsilon,eff}}$	1	$-\frac{\varepsilon}{K}\left(C_1 S_K - C_2\rho\varepsilon\right)$
g	1	$\frac{\mu_{eff}}{\sigma_{g,eff}}$	1	$-\left(C_{g_1} G_{g_2} - C_{g_2}\rho\frac{\varepsilon}{K} g\right)$

Further details of the mathematical models may be found in the literature [13-15].

Turbulent combustion models

The equations for the species concentration and the species concentration fluctuation represent the combustion processes and will be referred to the combustion model. There are three main combustion models [18]. But for the sake of accuracy and the form of turbulence equation (by Eq. (2)), only one of them is considered here. In this model, the fuel inlet is surrounded by the oxidant inlet as an annular orifice, the reaction is one step with fuel and oxidant unable to coexist at the same location, and with the assumption of infinitely fast chemistry (physically controlled), according to the following reaction equation:

1 kg fuel + i kg oxidant $\rightarrow$ (1+i) kg products (3)

By manipulating of the obtained species conservation equations for fuel and oxidant in the general form of Eq. (1) and according to Eq. (3), firstly the equation of φ_{fo} and finally the equation of mixture fraction f are derived. By evaluating f as the only species equation to be solved, the instantaneous species mass fraction is completely determined by [19]:

$$f = \frac{\varphi_{fo} - \varphi_{fo,o}}{\varphi_{fo,F} - \varphi_{fo,o}} \quad (4)$$

Where:

$\varphi_{fo} = m_{fu} - \frac{m_{ox}}{i}$; f=0(for inlet oxidant) and f=1 (for inlet fuel); $m_{fu} + m_{ox} + m_{pr}$=1

Radiation models

Thermal radiation enters as a source term in the enthalpy equation. For the evaluation of this term, radiation models are introduced. Thermal radiation is normally governed by an increasingly complex procedure, involving a coupling of the integral equations

of the zone method to the differential equation of the flow, chemical reaction, and heat transfer. A simpler method is to replace the integro-differential equation by a system of differential equations using a flux approximation method [20].

The advantages which this transformation brings are twofold. First, the differential equations can be solved by standard finite difference techniques; and second, the finite difference equation are of the space "sparse matrix" kind, where in a zone temperature, it is linked only to its immediate neighbors. Corresponding to one, two and three dimensional coordinate system, there are two, four and six flux models respectively. In the present research, a four flux model is used; therefore, equations of model are written for the rate of change of positive radiation fluxes I and J in the positive and negative coordinate directions.

In the absence of scattering, they are, for the axial direction [20]:

$$\frac{d(I_z)}{dZ} = -a \cdot I_z + a \cdot E \quad (5)$$

$$\frac{d(J_z)}{dZ} = -a \cdot J_z + a \cdot E \quad (6)$$

And for the radial direction:

$$\frac{d(rI_r)}{dr} = r\left[-a \cdot I_r + \left(\frac{J_r}{r}\right) + a \cdot E\right] \quad (7)$$

$$\frac{d(rJ_r)}{dr} = r\left[a \cdot J_r + \left(\frac{J_r}{r}\right) - a \cdot E\right] \quad (8)$$

The working equations may be resulted with the combination of each pair of first order flux equations to yield a single second order equation:

$$\frac{d}{dZ}\left[\Gamma_z \frac{d(F_Z)}{dZ}\right] + a(E - F_z) = 0 \quad (9)$$

$$\frac{1}{r}\frac{d}{dr}\left[\Gamma_r \cdot r \frac{d(F_r)}{dr}\right] + a(E - F_r) = 0 \quad (10)$$

Finally, the source term in the enthalpy equation is, as follow:

$$S_R = 2a(F_z + F_r - 2E) \quad (11)$$

Where [18]:

$$a = 0.2m_{fu} + 0.1m_{pr} \quad (12)$$

Further detail of this model can be found in Ref. [20]. These are the working equations, which cast into finite difference form; and the calculation of the radiation fluxes are embedded in the iteration cycle employed for the other variables.

Boundary conditions

The elliptic form of the conservation equations represented by Eq. (1) necessitates the specification of boundary conditions for each surface of the solution domain. This domain is a symmetrical half section of the furnace and a symmetry condition is, therefore, imposed on the axis. The solid furnace and tube walls, inlet and outlet boundary conditions can be found in the Refs. [13, 18, 20].

NUMERICAL MODELING

The differential equations based on Eq. (1) were expressed in the finite difference form by integrating over finite areas, together with assumptions about the distributions of the variables between the nodes of the grid [13]. Doing this, it enables us to ensure that conservation laws are obeyed over arbitrarily large or small points of the field. Also this procedure lends itself better to physical interpretation, and hence is easier to understand. By recasting of the finite difference equations, the successive substitution formula is derived.

It should be noted that, the software can apply the differential equations in any generally applicable form, expressible in terms of any curvilinear-orthogonal coordinate system. Usually, either because the equations are very numerous, or because of non-linear ties, iterative methods must be employed to solve the algebraic equations. We have chosen the method known as "point successive over relaxation" [13, 21]; and it is known in certain circumstances to be more rapid than the Gauss-Seidel method.

Combustion of a natural gas fuel in an existing (conventional) vertical furnace with a single-type burner as discussed in Ref. [22], i.e., as illustrated in Fig.1 and Table 2, was studied numerically under the high temperature and low oxygen content exhaust gases as well as HPDAC and conventional combustion conditions for several cases. Since no experimental data are available in the literature; the success of the calculation procedure is checked by the qualitative and quantitative verification of the high temperature and low oxygen

Table 2: Information of the existing industrial furnace.

Geometrical data	
Length (m)	9.272
Diameter (m)	3.048
Tubes number	48
Tubes Outside diameter (m)	0.1143
Tubes Inside diameter (m)	0.093
Tubes spacing (m)	0.2032
Burner type	Center, single
Process data	
Fuel type	Natural gas
Oxidant type	Air, 21% O_2
Process fluid inlet temperature (k)	783.15
Process fluid flow rate (kg s^{-1})	45.1811
Air inlet temperature (k)	300
Excess air (%)	10
Fuel flow rate (kg s^{-1})	0.1745
Fuel wetness (%)	0.0
Fuel net heating value (kj kg^{-1})	51234
Fired heat (mega watt)	8.939

content exhaust gases/HPDAC and conventional (low and high air temperature) combustion results through the comparison of them with the results reported in the literature and the zone model results [14], respectively. The variables chosen for numerical studies are represented by Table 3, and the present calculations were performed for a symmetrical half section furnace as the computational domain with a grid composed of 21 in 21 and 71 in 71 nodes and with allowing the solution of six equations (corresponding to ω/r, ψ, f, h, F_z and F_r). The spacing between the nodes was adjusted to concentrate the nodes in the regions with steep variations.

It should be noted that, for simulation of the low oxygen content exhaust gases/HPDAC combustion, a steady state process is assumed in which the exhaust/firing cycles will not be reversed and therefore half a burner cycle was calculated.

A full description of the method is beyond the scope of this paper, so for the details of the numerical solution the reader is referred to Refs. [13, 18, 20].

Several case problems have been solved and the following measures have been taken to avert the divergence of the solution:

- Near the wall; the ratio of the intervals between the nodes should be kept constant as possible; in fact there is reason to believe that this ratio should not exceed 1.5.

- The wall vorticity should be removed from the substitution formula for the near-wall nodes. In fact the wall vorticity does not appear explicitly; therefore this variable need only be calculated at the end of the iteration process.

- By using the "under-relaxation parameter", which stands for a number between 0 and 1, for a variable which varies most widely from one iteration to the next.

- By reducing the variations in the source term of the substitution formula, when this term is a function of dependent variables.

The accuracy which can be obtained with any finite-difference method of solution is closely tied up with the truncation error. By reduction the (tetrahedral) mesh size, this kind of error can be reduced. As can be seen from Table 3, the average relative difference between the overall results of case 4 (with 441 grid nodes) and case 5 (with 5041 grid nodes), which are exactly the same, is about 2%; and between the overall results of case 1 (with 441 grid nodes) and the zone model case (with 80 surface and volume zones) [22], also between the real[22] and the predicted bridge wall temperature value of these two latter cases are about 10%, 0.7% and 4.1%, respectively. These comparisons of results indicate the low truncation and round-off errors of the present model and that its accuracy is higher than the zone model.

We know that the number of grid nodes, the initial conditions for variables and the nature of the boundary conditions are the factors which influence the economy of the calculation procedure. So in this work by applying the over-relaxation parameter and the variable grid spacing; also avoiding the specification of the normal gradient at boundaries when possible, the computation time has been decreased. For example, the average CPU-time needed for computation the cases presented in Table 3, are in the range of 3 second (for the cases with 441 grid nodes number) to 5.75 minutes (for the cases with 5041 grid

nodes number) on a "Pentium 4 with 3.00 GHZ CPU and 512 MB of RAM "machine.

Furthermore for analyzing the results of numerical simulation, the parameters of chemical flame size, gas temperature uniformity ratio and flame peak temperature were defined and used as the HPDAC'S main unique features achievement criteria, as follow:

The HPDAC'S Main Unique Features Achievement Criteria

Chemical Flame Size

Determination of flame size is useful to optimize the size of the combustion chamber or to determine the optimal number of flames per combustion chamber. Traditionally the flame boundary is defined as the surface at which combustion is complete. However, because combustion is normally very fast, the boundary represents the area at which the fuel and the oxygen ratio is stoichiometric. The HPDAC flame is less luminous or even flameless, thus its size is not so clearly defined and is difficult to measure and in a sense it can be said that the HPDAC combustion is more like"volume combustion". Therefore, the flame length is not enough to characterize the flame size. So in this work the "stoichiometric mixture fraction" parameter (f_{st}) has been used for describing the flame border [11, 19]. It should be noted; it is supposed that thermodynamic equilibrium prevails throughout the defined combustion model of this work. This means that finite values of both fuel and oxygen concentration can not prevail at the same point. So, for φ_{fo} values of Eq. (4) in excess of zero, φ_{fo} equals m_{fu}; and for φ_{fo} values below zero, it equals $-m_{ox}/i$.

The condition $\varphi_{fo} = 0$ ($= m_{fu} = m_{ox}$) is the special one known as "stoichiometric"; the front of the chemical reaction, i.e., the flame envelope, is the locus of all points for which φ_{fo} equal zero. By applying the above condition in Eq. (4), we obtain:

$$f_{st} = \frac{1}{1+i} \tag{13}$$

Thus, the flame volume can be approximately defined when $f_{st} \le f \le 1$.

Gas Temperature Uniformity Ratio

Numerous works in the literature state that the HPDAC combustion gives much more uniform temperature field than traditional combustion. Gas temperature uniformity ratio (GTUR) is used to describe the gas temperature field uniformity inside the furnace as defined below:

$$GTUR = \sqrt{\frac{\sum_{x=1}^{x=n}\left(\frac{T_x - \bar{T}}{\bar{T}}\right)^2}{n}} \tag{14}$$

When GTUR=0, there is no gas temperature gradient inside the furnace.

As can be seen from Table 3, the advantage of the above equation is that, GTUR value is independent of the grid nodes number (for instance, with comparison of its same value for cases 4 and 5). In other word, by eliminating the parameter "n" from the Eq. (14), we have an equation [10] that, if it is used for the above mentioned cases (which, except of their grid nodes number, they are exactly the same), the different GTUR values can be obtained.

Flame Peak Temperature

The higher flame temperature occurs, whereas the flame envelopes. At the flame peak temperature, it is assumed that the radiation fluxes can be neglected respect to convection fluxes. So, the source term of energy equation S_R vanishes and it is then easy to deduce from the similarity of the mixture fraction and energy equations and their boundary conditions that *f* and h must be linearly related as follow:

$$f = \frac{h - h_o}{h_F - h_o} = \frac{\varphi - \varphi_{fo,o}}{\varphi_{fo,F} - \varphi_{fo,o}} \tag{15}$$

Thus from Eqs. (13) and (15), we obtain:

$$T_{f,max} = \frac{\left(CP_F/CP_{pr}\right)\cdot T_F + \left(h_F/CP_{pr}\right) - \left(CP_O/CP_{pr}\right)\cdot T_O}{1+i} + \left(CP_O/CP_{pr}\right)\cdot T_O \tag{16}$$

The simulation results, which have not been presented here, show that the average relative difference between the flame peak temperature calculated from the energy equation and the Eq. (16) is about 4%. This implies that, the above assumption can be correct. As can be found from the Eq. (16), for any oxidizer and fuel temperature, the flame peak temperature decreases with the reduction of oxygen concentration, i.e., the increasing of i, for oxidizer.

Table 3: The simulation results of the several cases study.

	Zone model	Present model								
		Case 1	Case 2	Case 3	Case 4	Case 5[a]	Case 6	Case 7	Case 8	Case 9
Fuel Type, %vol	Natural gas	Natural gas	Natural gas	Natural gas	Natural gas	Natural gas	Natural gas	Natural gas	Natural gas	Natural gas
Air/Fuel Stoichiometric Ratio, (kg/kg)	16.5	16.5	16.5	35.5	35.5	35.5	35.5	35.5	35.5	35.5
Air Temp After Regenerator, (K)	300	300	1273.15	1273.15	1273.15	1273.15	1273.15	1273.15	1273.15	1273.15
Air Temp Before Regenerator, (K)	300	300	300	300	300	300	300	300	300	300
Fuel Temp, (K)	300	300	300	300	300	300	300	300	300	300
Oxygen Concentration of Air, (% vol)	Air , 21%	Air , 21%	Air , 21%	Air , 10%	Air , 10%	Air , 10%	Exhaust gas, 10%	Air , 10%	Exhaust gas, 10%	Exhaust gas, 10%
Excess air, (%vol)	Air , 10%	Air , 10%	Air , 10%	Air , 10%	Air , 10%	Air , 10%	Exhaust gas, 10%	Air , 10%	Exhaust gas, 10%	Exhaust gas, 10%
Fuel Flow Rate, (kg s^{-1})	0.1745	0.1745	0.1745	0.1745	0.1222	0.1222	0.1222	0.1222	0.1222	0.1745
Fuel Velocity, (m s^{-1})	-	1.91	1.91	1.91	1.34	1.34	1.34	1.34	1.34	1.91
Air Velocity, (m s^{-1})	-	10.91	22.51	22.75	15.93	15.93	15.93	7.58	7.58	22.75
Outlet Flue Gas Velocity, (m s^{-1})	-	5.58	4.69	9.27	6.29	6.04	6.02	6.65	6.3	8.69
Residence Time of Furnace Flow, (s)	-	4.763	5.667	2.868	4.226	4.398	4.42	4.0	4.221	3.06
Momentum Flux Ratio	-	0.13745	0.13726	0.13725	0.13725	0.13725	0.13725	0.28849	0.28849	0.13725
Fired Heat, (mega watt)	8.939	8.939	8.939	8.939	6.258	6.258	6.258	6.258	6.258	8.939
Process Fluid Inlet Temp, (K)	783.15	783.15	783.15	783.15	783.15	783.15	783.15	783.15	783.15	783.15
Process Fluid Outlet Temp, (K)	801.6	798.37	813.97	802.14	800.55	799.53	796.96	804.63	803.18	797.22
Furnace Efficiency, (%)	39.01	38.653	78.254	48.236	63.114	59.425	50.094	77.894	73.419	37.01
Required Regenerator Efficiency, (%)	0.0	0.0	92.99	104.2	109	109	108.6	100.8	101	107.1
FLUE GAS TEMP BEFORE REGENERATOR , (K)	1485.93[b]	1437.48	1198.86	1125.3	1088.9	1089.7	1036.5	1153.3	1091.84	1046.8
Flue Gas Temp After Regenerator, (K)	1485.93	1437.48	362.8	265.2	228.8	229.6	236.3	293.3	291.6	246.6
Max & Mean Gas Temp of Combustion Chamber, (K)	1817 1338	2347 1410	3201 1552	2132 1352	2128 1323	2164 1323	1933 1256	2082 1310	1882 1257	1935 1263
Gas Temp Uniformity Ratio, (%)	-	31.36	32.92	24.366	24.192	24.242	22.474	20.852	19.69	22.564

a) Result according to increasing of 12 times grid nodes number, respect to case 4.
b) Actual (operating) value of bridge wall temperature=1427.59 K.

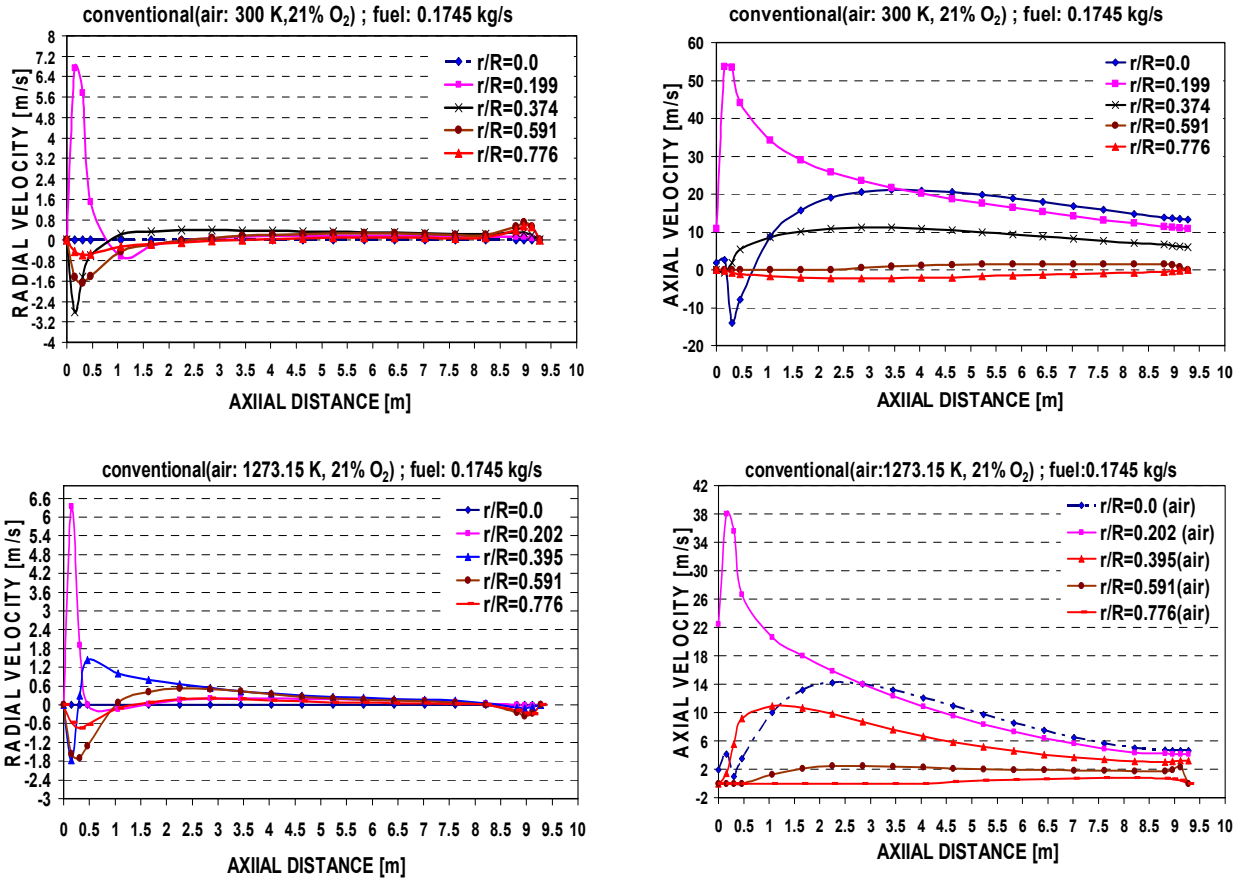

Fig. 2: Axial and radial gas velocity profiles under the different conventional combustion conditions.

RESULTS AND DISCUSSION

The simulation was carried out under several cases of the low oxygen content exhaust gases as well as HPDAC and conventional combustions, as illustrated in Table 3, in order to study the flow and heat transfer properties under the above mentioned conditions for investigating the possibility of using high temperature and low oxygen content exhaust gases as oxidant instead of HPDAC for combustion in an industrial furnace. The momentum flux ratio [12] and velocity ratio [23] between the fuel gas jet and the air/oxidant flows are part of the conditions that were maintained constant for some of the cases studied. This provides a similarity in the mixing of fuel and air/oxidant streams. Using this procedure, it is possible to identify the net effects of combustion air preheat temperature and oxygen concentration. In other word, the simulated results can be related to the combustion process itself.

Velocity distribution

For the flow properties, i.e., velocity components, distributions illustrated in Figs. 2 & 3, no experimental data are available for the comparison. However, it should be noted that, the trends of these results are in good agreements with those reported in the literatures such as Refs. [12, 18, 24]. As can be seen from the above mentioned figures, the distributions of the mean axial and radial velocities are very complicated. The corresponding fluctuations of the velocity are comparatively large close to the burner, i.e., the reaction zone, and tend to a uniform and lower value at down stream locations.

As can be seen from Figs. 2, 3 & 9, the maximum velocity corresponds to the flame peak temperature [12]. Recirculation zones which correspond to the negative values of velocities are related to the high temperature and correspondingly low values of density used in the solution of the momentum equation for the hotter regions of the flow. In the near wall regions, due to the lower values of the temperature and the correspondingly high value of density, and therefore more effects of the gravity force, the flow circulate downward.

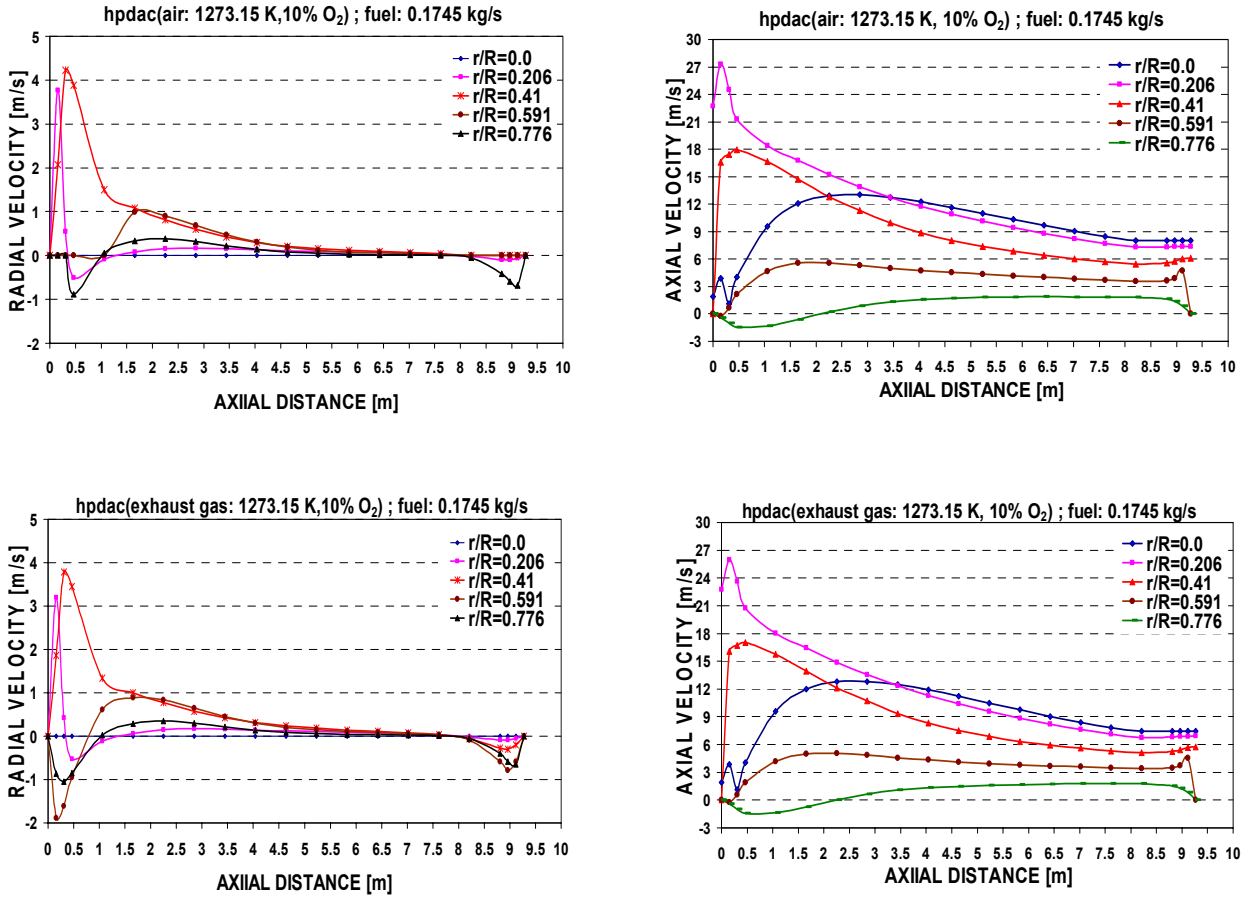

Fig.3: Axial and radial gas velocity profiles under the different HPDAC combustion conditions.

When the combustion- air preheat temperature or its oxygen concentration are decreased, the reaction rate is slower, thus the jet expansion occurs over a larger volume, in both axial and radial directions and finally the lower velocities are obtained under the condition of the same momentum flux ratio and the same velocity ratio between the fuel gas jet and air flow. As can be seen from Table 3 and Fig.3, due to the higher heat capacity value for the cases with exhausted gas as oxidizer, it is interesting that their maximum flame temperature are slightly lower than those for the cases with diluted air as oxidant, i.e., their velocity are slightly lower than those for diluted air. This result is in a good agreement with the reported results in literature [10, 12, 23, 25, 26].

Fuel and air mass fraction distribution

As can be seen from Figs. 4 and 5, most of the combustion takes place in the central zone of the furnace and is distributed according to the furnace inside flow pattern. Oxygen concentration decreases close to the flame and falls to the minimum value at the center line of combustion chamber. Also it can be assumed that the flame borders are located in the place where the oxygen level begins to fall from its initial value. In this case, it can be noticed that for lower oxygen content the flame is wider and its volume bigger. The steeper curve slope for fuel/air mass fraction means more intense reaction [10]. Moreover, the higher width and length of the combustion zone or in other words the reaction volume vary as HPDAC-exhaust gas>HPDAC-diluted air>conventional combustion. This result is in a good agreement with the reported results [8, 10, 11, 12, 14, 25, 26].

Temperature distribution

As can be seen from Table 3 and Figs. 6 & 7 for conventional combustion (low temperature air combustion),

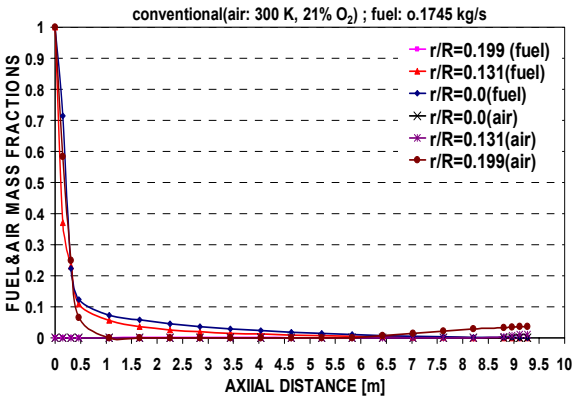

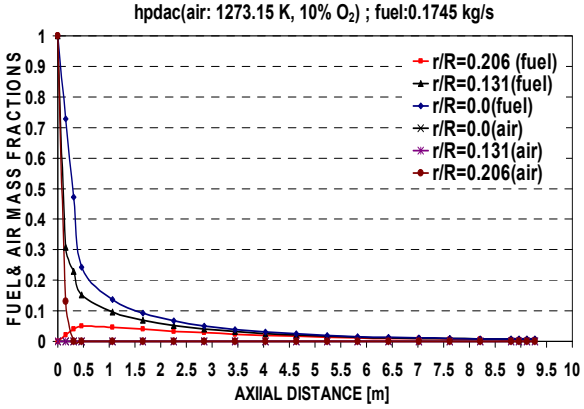

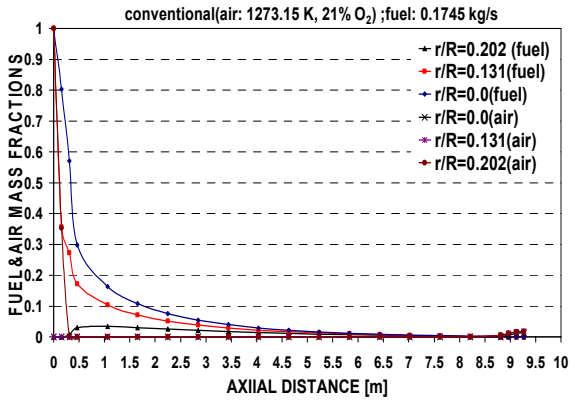

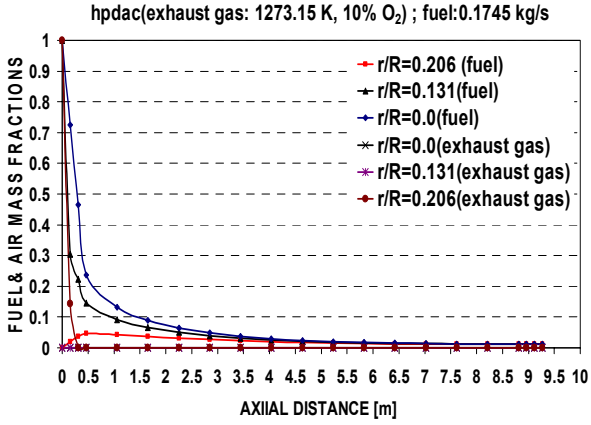

Fig.4: Fuel and air mass fractions distributions under the different conventional combustion conditions.

Fig.5: Fuel and air mass fractions distributions under the different HPDAC combustion conditions.

the tube wall, process fluid and gas temperature distributions results of the zone model [22] and the present model are in good agreements. The corresponding fluctuation in temperature is comparatively large close to the burner, i.e., the reaction zone, and tends to have uniform and lower values at the down stream locations.

The location of maximum temperature fluctuation corresponds approximately to the end part of the luminous flame zones; and the maximum discrepancies between the present model and the zone model are at the reaction zones according to the combustion model considered. From Fig.8, it can be seen that the higher tube wall temperature uniformity vary as HPDAC-exhaust gas>HPDAC-diluted air>conventional combustion. As illustrated in Table 3 and Figs. 9, 10 & 11, for any preheated oxidizer temperature, by the reduction of its oxygen concentration, the flame peak temperature calculated from Eq. (16) and thus, the gas temperature non-uniformity decreases. When the oxidizer temperature is increased, the zone of high temperatures tends to shrink; thus, a more intensive reaction takes place. In addition and as it was explained before, the thermodynamic limitations to the maximum temperature of the HPDAC combustion, the larger reaction volume and thus the low maximum local heat release rate, result in this uniform and relatively moderate temperature profile and hence the suppression of thermal-NO formation in the HPDAC combustion respect to conventional combustion [10, 12, 25].

As can be seen from Fig. 11 and Table 3 for cases 3 and 9, due to the higher heat capacity value for the cases with exhausted gas as oxidizer, it is interesting that their maximum flame temperatures and thus their gas temperature uniformity ratios (which inversely related to gas temperature uniformity), are slightly lower than those

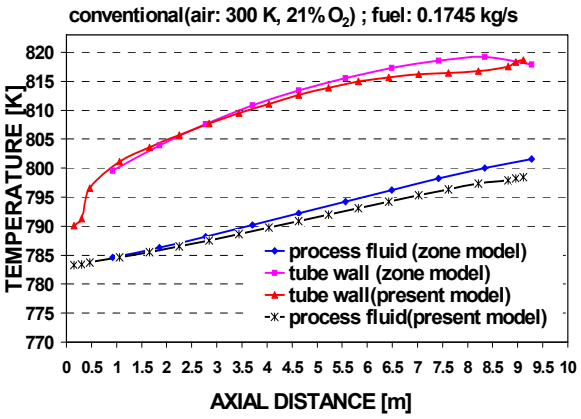

Fig. 6: Tube wall and process fluid temperature distributions under the conventional combustion condition for the zone and present models.

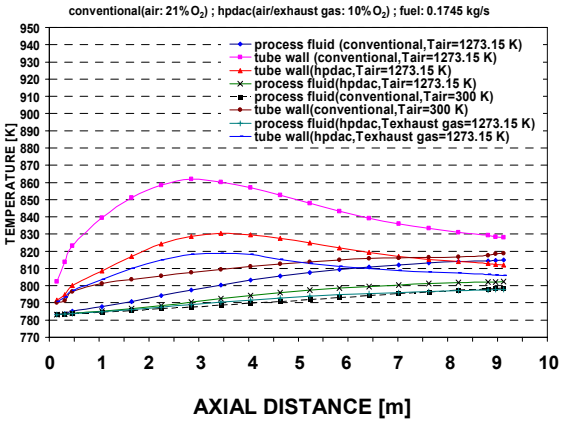

Fig. 8: Tube wall and process fluid temperature distributions under the different conditions of conventional and HPDAC combustions for the present model.

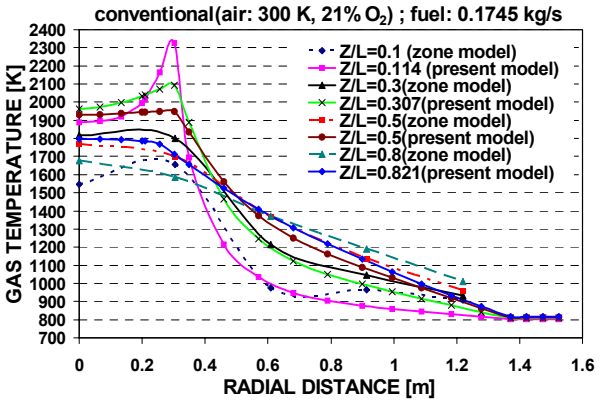

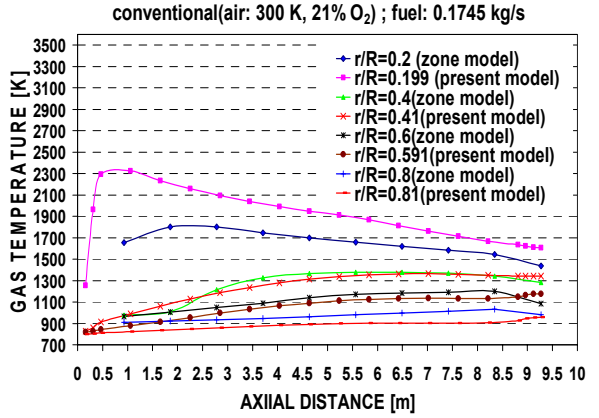

Fig.7: Axial and radial gas temperature distributions under the different conventional combustion condition for the zone and present models.

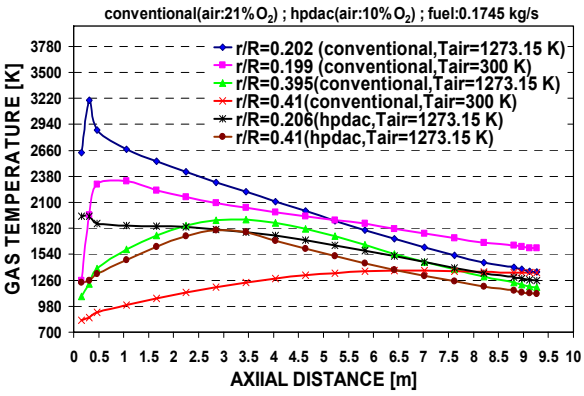

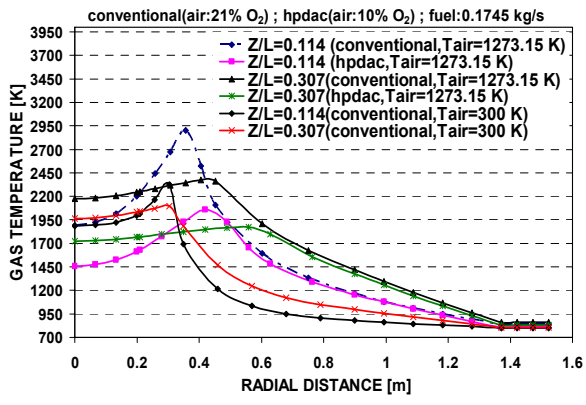

Fig. 9: Axial and radial gas temperature distributions under the different conditions of conventional and HPDAC combustions for the present model.

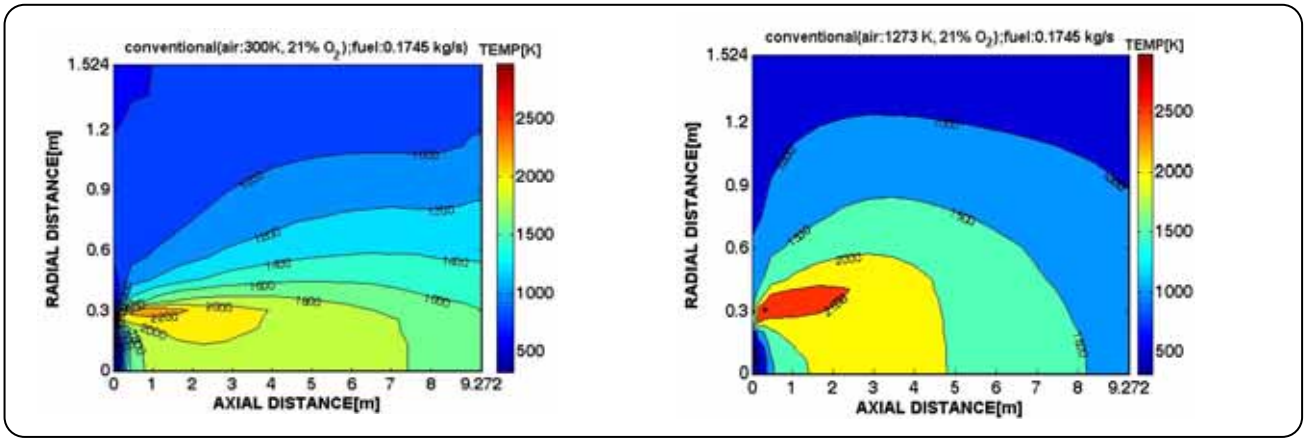

Fig.10: Gas temperature distributions under the different conventional combustion conditions for the present model.

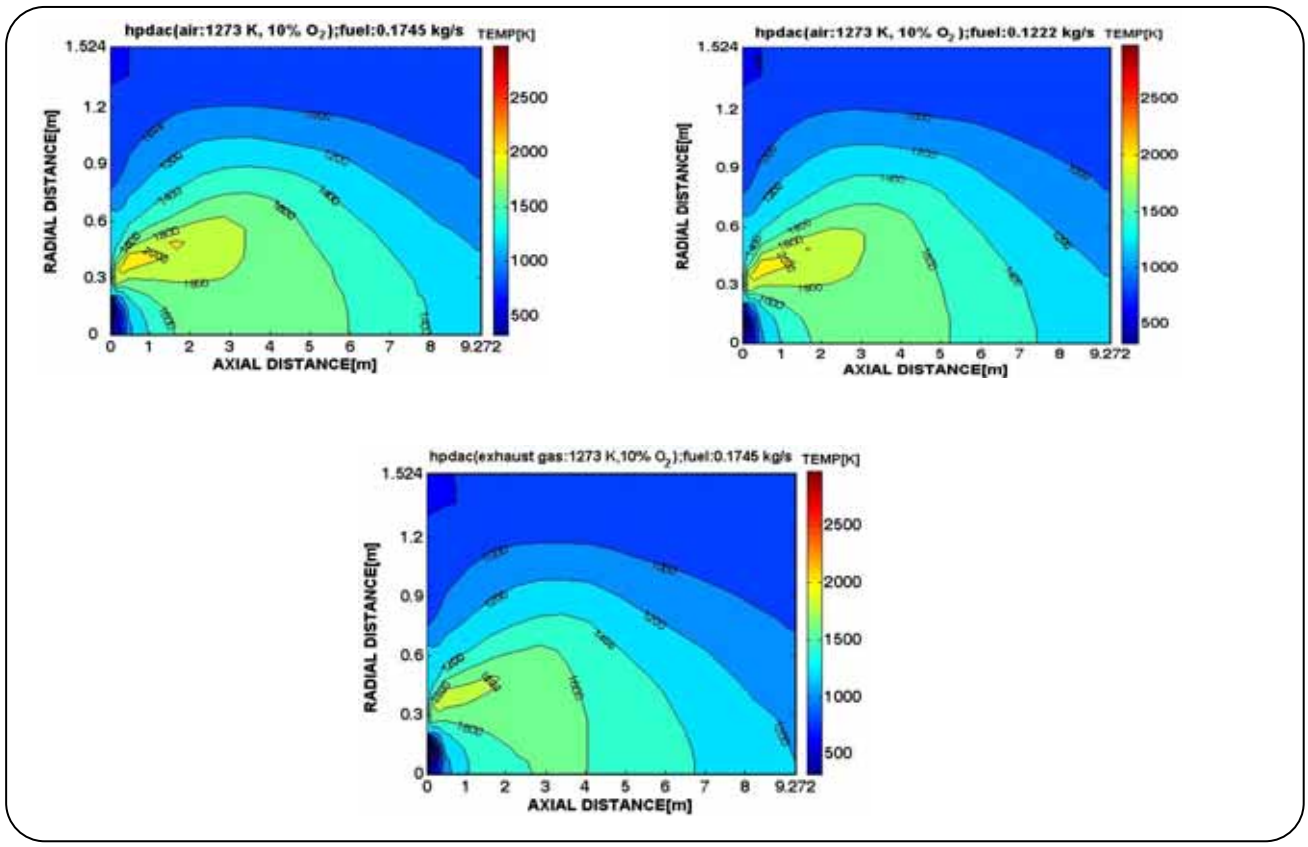

Fig.11: Gas temperature distributions under the different HPDAC combustion conditions for the present model.

for diluted air [26]. Also Table 3(for cases 4, 6, 7 and 8) shows that a lower ratio of fuel to oxidant injection momentum leads to a larger flame peak temperature and thus a larger NO production [12]. This phenomenon is slightly stronger for exhausted gas than diluted air as oxidizer. In addition the trend of the results presented here, are in a good agreement with the results reported in Refs [8, 10, 12, 22, 25, 26].

Heat flux distribution

As can be seen from Fig.12 for conventional combustion, the tube wall total heat flux profiles results of the present

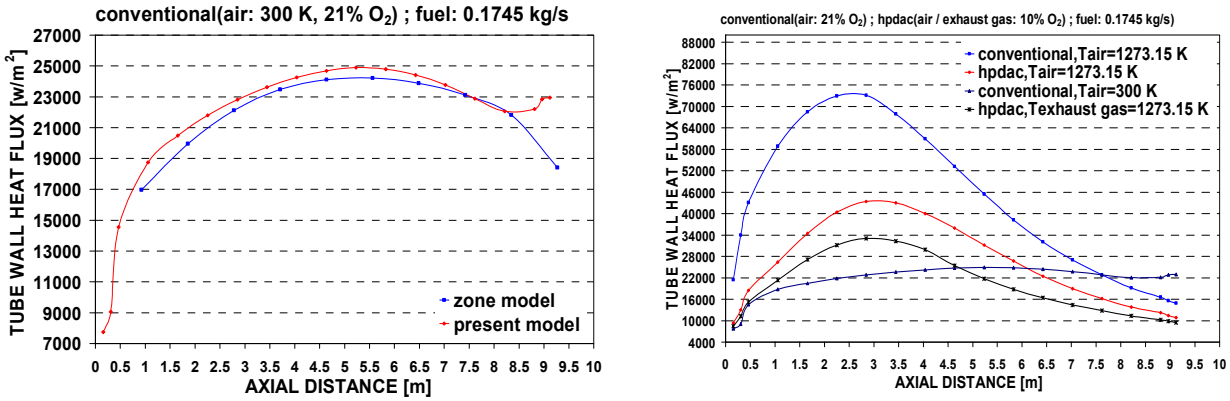

Fig.12: Tube wall total heat flux distributions under the different conditions of conventional and HPDAC combustions for the zone and present models.

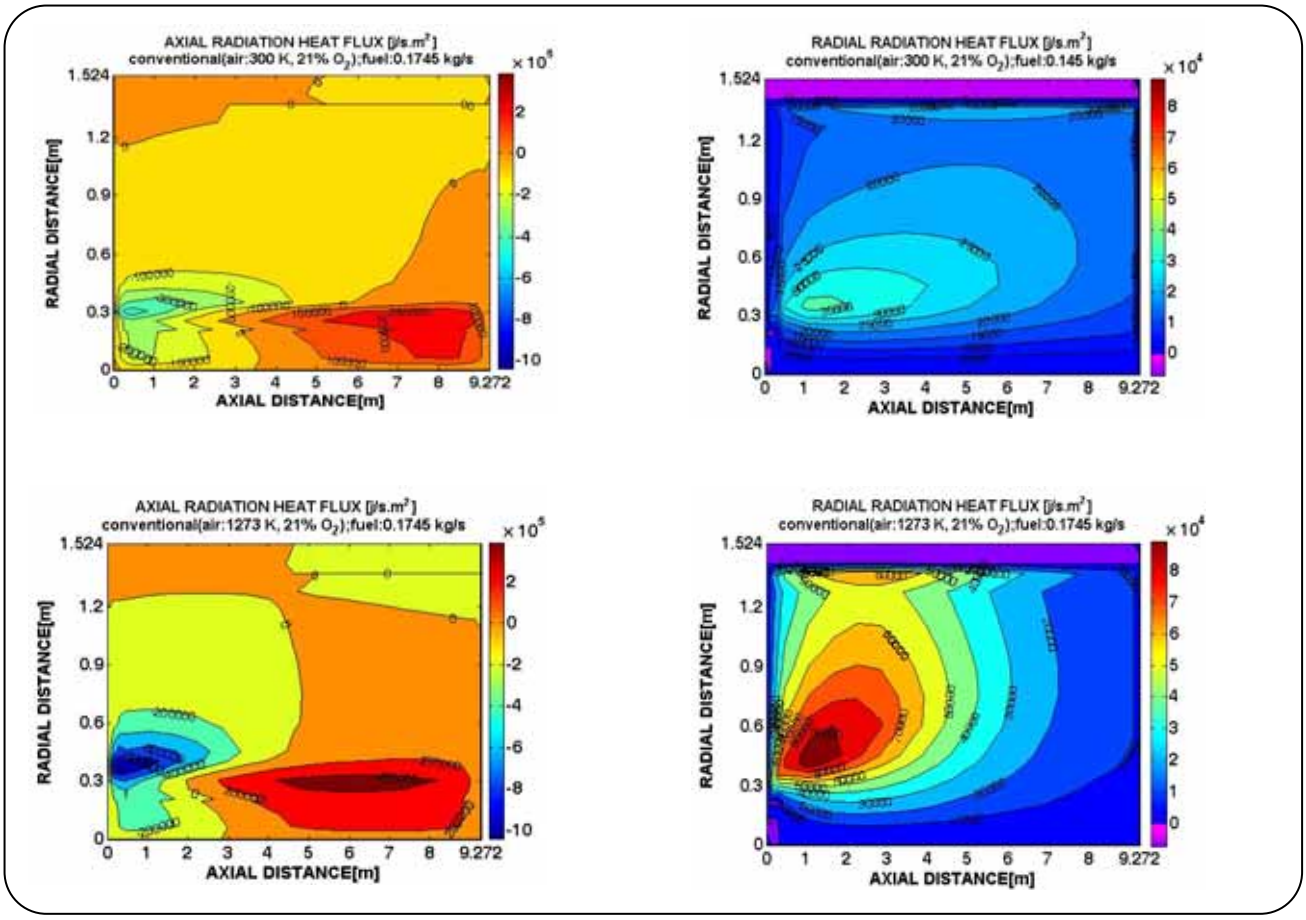

Fig.13: Axial and radial gas radiation net heat flux distributions under the different conventional combustion conditions.

work and those of the zone model [22], and those from Fig.13, the trend of the radiation net heat flux profiles for gas field in radial and axial directions, are in good agreement with the results reported in Refs [6, 14, 20]. It is interesting to note that for the conventional combustion, 96% of the total heat flux on the tubes is related to the radiation and only 4% are from convection heat transfer. This is also validated when compared with the results reported in Ref. [22]. In spite of the moderate-uniform temperature profile of the gas field (Fig. 9),

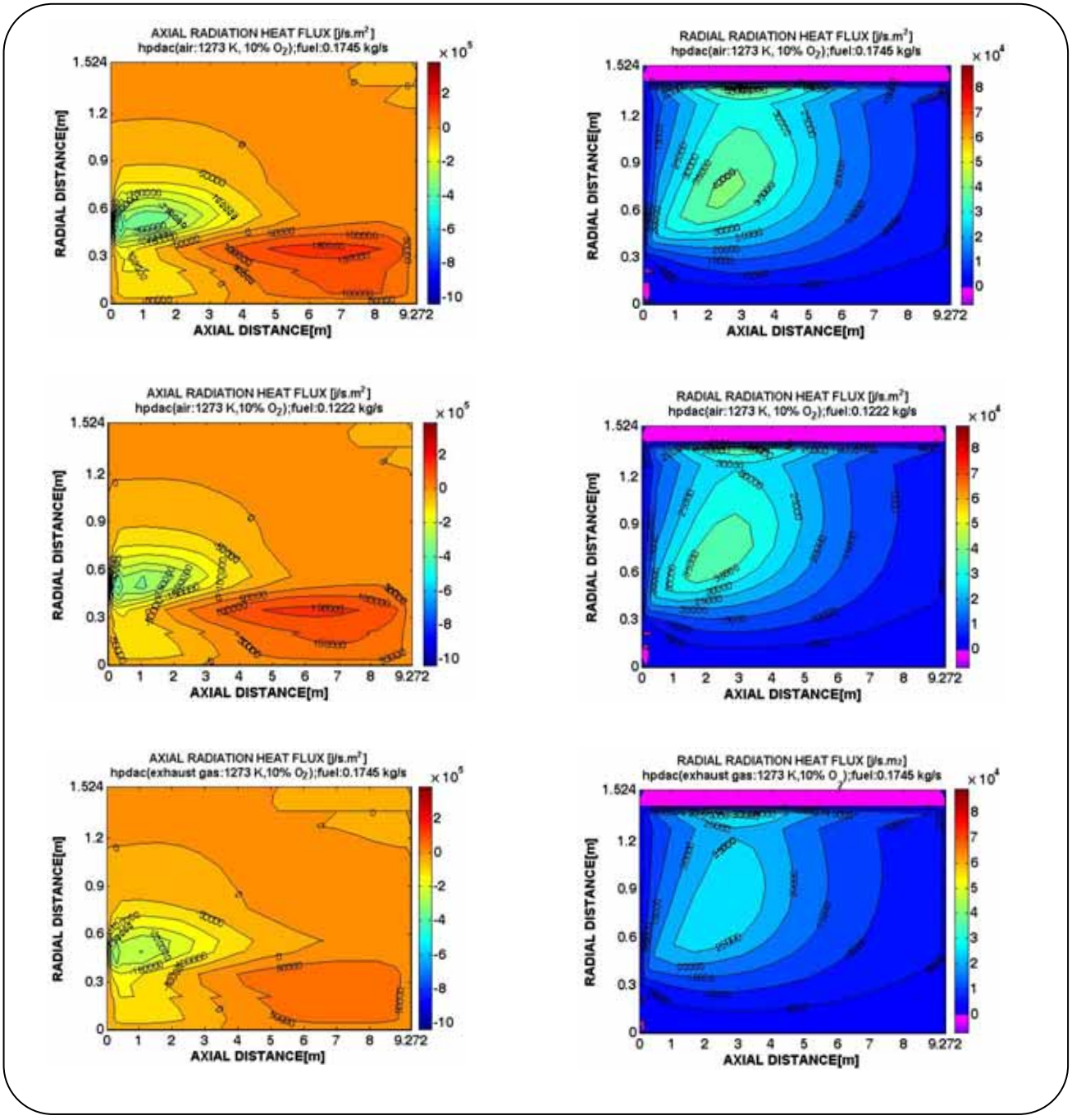

Fig.14: Axial and radial gas radiation net heat flux distributions under the different conditions of conventional and HPDAC combustion conditions.

as can be seen from Figs. 12, 13 & 14, the flame under the HPDAC combustion condition with the diluted air/exhaust gas as oxidant, has a more uniform heat flux and emits more thermal radiation to its surrounding, i.e., the gas field and the tube skin, than the conventional flame (low temperature). This phenomenon can be translated into uniform heating of the material to be heated and reduced energy requirements, consequently suppressing CO_2 and thermal-NO formations. It should be noted that, the negative values of radiation net heat flux are related to the radiation heat transfer in the negative coordinate directions. The trends of these latter results are also validated when compared with the results reported in Refs. [12 , 27].

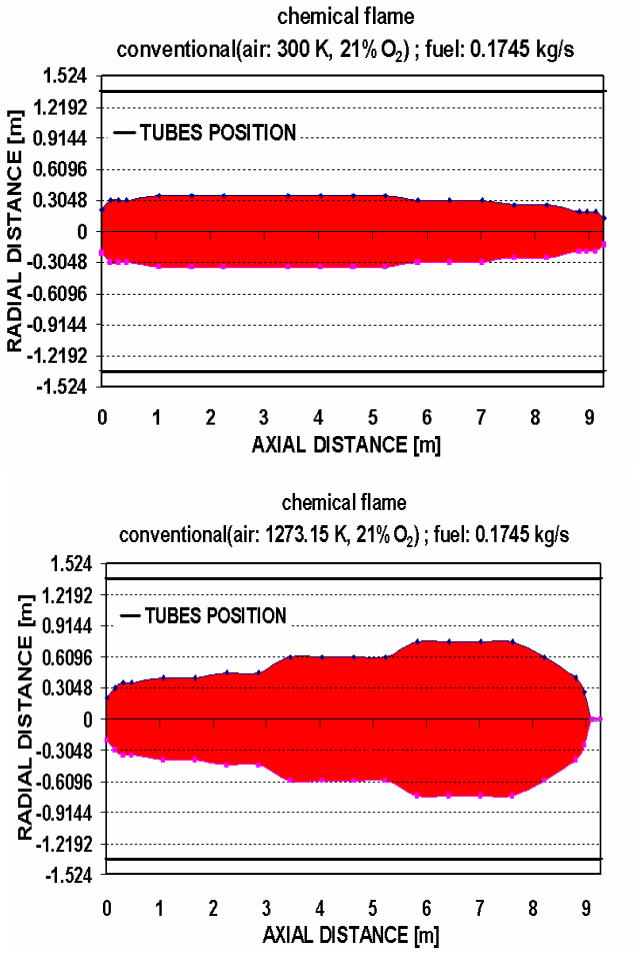

Fig.15: Chemical flame shapes under the different conventional combustion conditions.

Chemical flame volume

Using of Eq. (13) and the assumption that the flame volume is confined to the region where $f_{st} \leq f \leq 1$; Figs. 15 & 16 show the predicted chemical flame shape and volume. The flame zone is almost limited to the volume of the hypothetical cylinder created by the air jets, because of their strong injection momentum, and consequently resulting in a rather long flame. The predicted results are found to agree well with respect to the shape of flame zone in Refs. [8, 12, 27].

As can be clearly seen from Figs. 4 & 15, and Table 3, under conditions of the same momentum flux ratio and the same velocity ratio between the fuel gas jet and air flow, when an oxidizer of 21% oxygen is maintained and the preheat temperature is increased, the fuel to air density ratio increases and mixing becomes slower [23], thus we have a bigger chemical flame volume. Of course, because the velocity ratio for case 2 is higher than that of case 1, and consequently resulting in a shorter chemical flame length [23]. Also when the oxygen concentration is reduced and a high preheat temperature is maintained (Figs. 5 & 16), the reaction is less intense, and thus we have an increased reaction, i.e., the chemical flame, volume. As it was explained before, when the low oxygen content exhaust gases are used as oxidizer instead of the diluted air, due to the higher exhaust gas heat capacity value, the lower flame peak temperature is resulted. This means the slower reaction rate, consequently increasing in chemical flame volume [11, 26].

The trend of these results as illustrated in Figs. 15 & 16 for a physically controlled combustion model, specially, having a long flame for conventional combustion [22] as well as a maximum flame diameter occurring at the end of the flame (because of the only half a burner cycle calculation) for a kinetically controlled combustion model [8], are also validated when compared with the results reported in Refs. [8 , 28], i.e., as illustrated in Fig.17.

Furnace/regenerator thermal performance

As can be seen from Table 3, for the cases with exhausted gas as oxidizer (cases 6, 8 and 9), the furnace efficiency is lower by about 5-10% and the required regenerator efficiency is higher by about 0.5-2% compared to the HPDAC(cases 3, 4 and 7). Nevertheless, for cases 6, 8 and 9, the gas temperature uniformity is relatively higher and the mean and the maximum gas temperatures, i.e., thermal-No formations, are lower than those of cases 3, 4 and 7. In spite of the high furnace efficiency during high temperature conventional combustion (case 2) with respect to the ambient temperature conventional one (case 1), case 2 is undesirable, because of its non-uniformity and also the higher flame peak temperature by about 36%, which increases the thermal-NO formation.

Furthermore, to provide the world's energy-environmental requirements, if energy aspect is more important than the environmental one, the HPDAC combustion (case 3) is firstly selected instead of high temperature and low content oxygen exhaust gases (case 9) and conventional combustions(case 1). This results in higher energy saving, i.e., lowers CO_2 formation by about 10%. Moreover, if environmental aspect is more

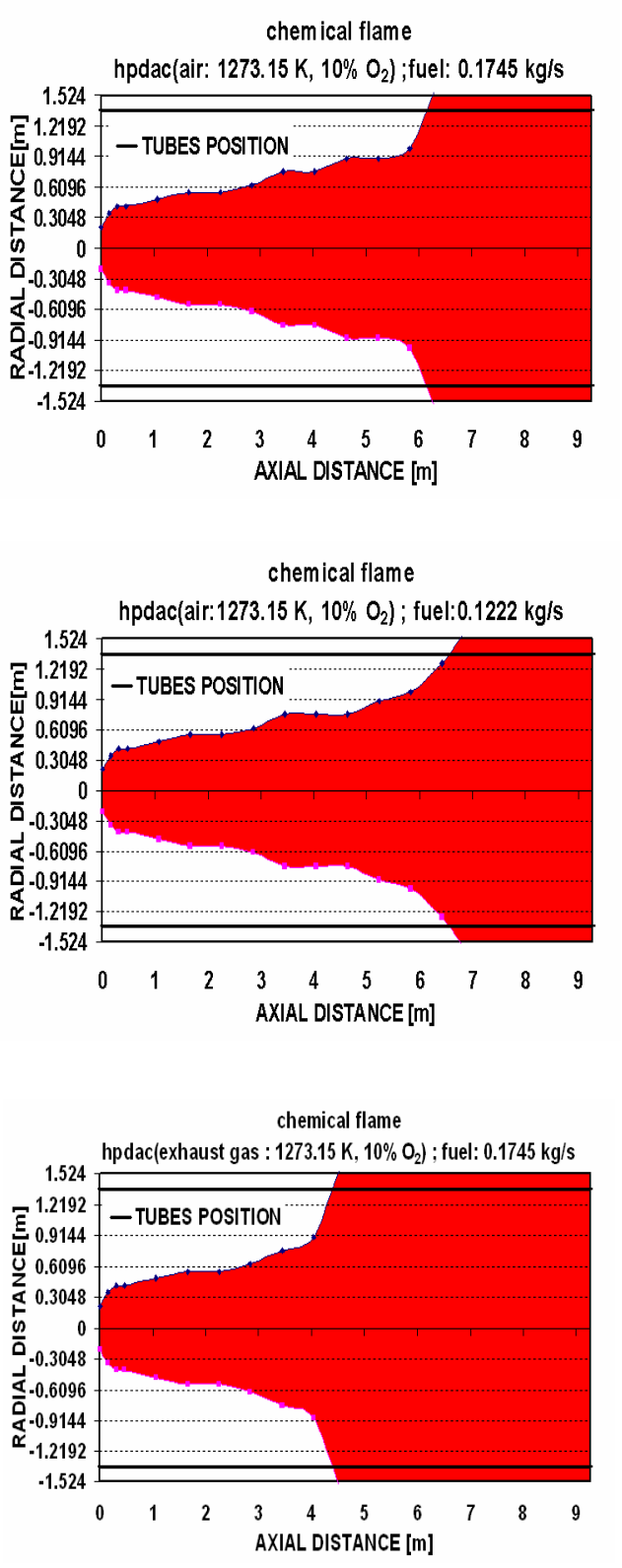

Fig.16: Chemical flame shapes under the different HPDAC combustion conditions.

serious, the preferred cases are the high temperature and low content oxygen exhaust gases condition. This result in lower flame peak temperature, i.e., lowers thermal-NO formation by about 9-19%. Finally for the best achievement of the world's energy requirement, an appropriate fuel flow rate (for example, the changing of case 3 to case 7) is selected, then there would be a system by about 30% lower fuel or energy consumption and a higher furnace efficiency by about 40%, i.e. the suppression of the CO_2 formation compared to the high temperature and low content oxygen exhaust gases combustion and conventional combustion(at ambient temperature) and a regenerator by around 3.4% lower required efficiency with respect to case 3. Also for the best achievement of the world's environmental requirement, an appropriate fuel flow rate (for example, the changing of case 9 to case 8) is selected, then there would be a system by about 30% lower fuel or energy consumption and a lower flame peak temperature by about 12-23%, i.e. the suppression of the thermal-NO formation with respect to high temperature and low content oxygen exhaust gases and ambient temperature conventional combustions and a regenerator by around 6.1% lower required efficiency with respect to case 9.

Low oxygen content exhaust gases or diluted air?

In summary and as it was explained before, if the low oxygen content exhaust gas is used as oxidizer instead of the diluted air (with the same temperature, oxygen concentration and flow rate), the exhaust gas-HPDAC's main unique features were better achieved than those of diluted air-HPDAC. In other word, the chemical flame volume increases and the gas temperature non-uniformity, the mean and maximum gas temperature and thus the thermal-NO formation will decrease. The trends of the results here are also validated when compared to the results reported in literature [11, 26].

CONCLUSIONS

- The quantitative verifications of the numerical simulation results of the present model for the industrial furnace described in Ref. [22] are only achieved under the conventional(low air temperature) combustion condition as follow: the relative differences between the predicted results of the present model and those of the zone model[22] equals ±0.4% for the process fluid outlet

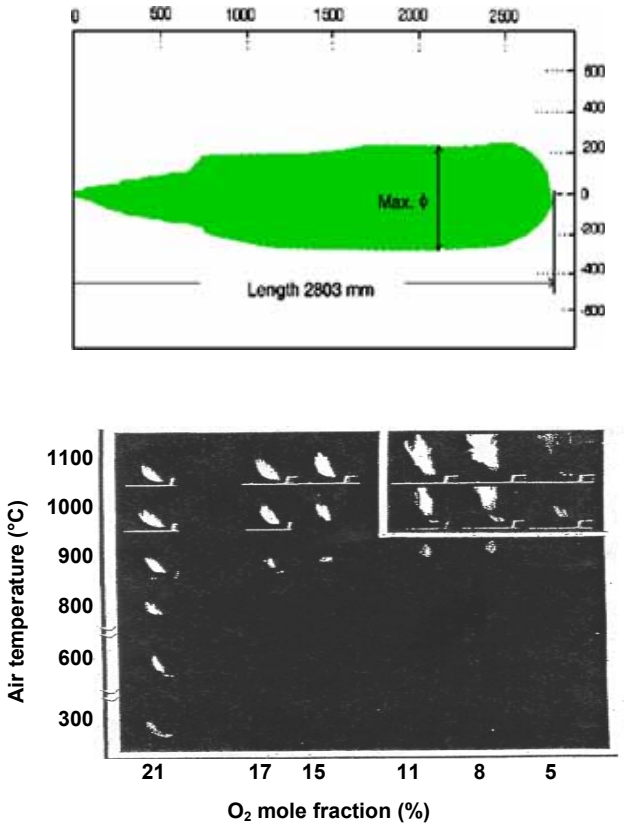

Fig. 17: Measured (HPDAC) [8] and direct photographs (conventional/HPDAC)[28] LPG flame shapes.

temperature; and ±0.9% for the furnace efficiency; and ±5% for the gas field mean temperature and finally between the actual (operating) bridge wall temperature and those predicted/calculated by the zone[22] and the present models equals ±4% and ±0.7%, respectively. Furthermore and according to Figs.6, 7 and 12, the other predicted results of the present model for tubes wall/process fluid temperature profiles, the gas field temperature profiles and the tubes wall heat flux profiles are also in very good quantitative agreements with those of the zone model. The qualitative verification of the obtained numerical simulation results of the present model are also checked firstly by comparison of them with the results reported in the literature under the relatively unusual HPDAC-diluted air and finally under the unusual HPDAC-low oxygen content exhaust gas. Under these conditions, there were encouraging agreements on the results' trends for the distributions of radial and axial gas velocities, and for the distributions of gas, process fluid and tubes wall temperatures. These harmonies, also existed for the distribution of fuel mass fraction, radial and axial net radiation heat fluxes, flame peak temperature as well as the gas temperature uniformity and finally for the chemical flame shape along with the furnace and regenerator efficiencies

- By application the exhaust gas as oxidizer instead of the diluted air, the chemical flame volume increases, and the gas temperature non-uniformity, the mean and the maximum gas temperature as well as the thermal-NO formation would decrease. In other word, the exhaust gas-HPDAC's main unique features were better achieved than those of diluted air-HPDAC.
- It may be concluded that, the present written computer program including the turbulence, combustion and radiation models as well as the concepts of the modified and proposed formula for defining the gas temperature uniformity, the chemical flame volume and the flame peak temperature be might able to represent and simulate the process of HPDAC with the low oxygen content exhaust gas as oxidant instead of the diluted air, for the furnace described in Ref. [22].

Acknowledgement

Corresponding author as a member of National Iranian Oil Company (NIOC) wishes to thank this company for its financial support and awarding Doctoral scholarship to him.

Nomenclature

a	Flux-model absorption coefficient (m^{-1})
C_1, C_2	Constants in turbulence model
C_{g_1}, C_{g_2}	Constants in combustion model
CP	Specific heat capacity ($J\ kg^{-1}K^{-1}$)
D	Furnace diameter (m)
E	Black body emissive power, δT^4 ($W\ m^{-2}$)
f	Mixture fraction
F	Radiation flux sum, (I+J)/2 ($W\ m^{-2}$)
g	Square of the fluctuation of concentration
G_{g_1}	Correlation related to g-equation
h	Stagnation enthalpy ($J\ kg^{-1}$)
h_F	Fuel calorific value ($J\ kg^{-1}$)
I	Positive radiation flux in the positive co-ordinate direction ($W\ m^{-2}$)
i	Air to fuel stoichiometric ratio ($kg\ kg^{-1}$)
J	Positive radiation flux in the negative co-ordinate direction ($W\ m^{-2}$)

K	Kinetic energy of turbulence per unit mass ($m^2 s^{-2}$)
k'	Constant equals 0.012
m	Mass fraction
$\dot{m}$	Mass flow rate (kg s^{-1})
n	Number of grid nodes
r	Radial distance from axis of symmetry (m)
R_{fu}	Rate of chemical reaction
S_k	Correlation related to k-equation
S_R	Source or sink of energy per unit volume and time associated with radiation
T	Absolute temperature (K)
$\overline{T}$	Mean absolute temperature (K)
V_1, V_2	Fluid mean velocity in the axial and radial direction respectively (m s^{-1})
V_3	Normal tangential velocity (m s^{-1})
V	Velocity (m s^{-1})
W	Furnace length (m)
Z	Axial co-ordinate along the furnace

Greek symbols

Γ_z, Γ_r	Equals 1/a and r/ (1+r.a) respectively (m)
μ_{eff}	Effective viscosity ($kg.m^{-1}.s^{-1}$)
ρ	Density (kg m^{-3})
δ	Stefan-boltzman constant (W $m^{-2}K^{-4}$)
σ_φ	Schmidt and prandtl number for any variable φ
ε	Dissipation rate of turbulent kinetic energy (m^2s^{-3})
φ	Dependent variable
ψ	Stream function
ω	Vorticity

Subscripts

eff	Effective (related to combined laminar and turbulent effects)
O	Oxidant stream
F	Fuel stream
f	Flame
fu	Fuel
ox	Oxidant
pr	Product
r	Radial direction
st	Stoichiometric
x	Grid nodes number indicator
z	Axial direction

Received : Nov. 6, 2008 ; Accepted : Jun. 22, 2009

REFERENCES

[1] Hasegawa, T., Tanaka, R. and Niioka, T., Combustion with High Temperature Low Oxygen Air in Regenerative Burners, Presented at the First Asia-Pacific Conference on Combustion, Osaka, Japan,12-15 May, pp. 290-293 (1997).

[2] Yasuda, T. and Ueno, C., Dissemination Project of Industrial Furnace Revamped with HTAC, Presented at the Second International Seminar on High Temperature Combustion in Industrial Furnace, Stockholm, Sweden, pp. 1-7(2000).

[3] Yang, W. and Blasiak, W., Combustion Performance and Numerical Simulation of a High Temperature Air-LPG Flame on a Regenerative Burner. *Scand J Metallurgy*, **33** (2), p. 113(2004).

[4] Ishii, T., Sugiyama, S. and Suzukawa, Y., Numerical Simulation of Temperature Distribution and NOX-Formation of Turbulent Diffusion Flame in High Temperature Air Combustion, Presented at the Japanese Flame Days 97, Osaka, Japan,16-17 May.(1997).

[5] Shimada, T., Uedo, M. and Imada, M., Computational Simulation of Regenerative Burner System and its Application to Walking Beam Furnace for Rolling Mill. *Industrial Heating*, **36** (2), 35(1999).

[6] Kobayashi, H. and Yoshikawa, K., Thermal Performance and Numerical Simulation of High Temperature Air Combustion Boiler, Proc. International Joint Power Generation Conference (IJPGC2000-15083), (2000).

[7] Dong, W. and Blasiak, W., Study on Mathematical Modeling of Highly Preheated Air Combustion, Presented at the Second High Temperature Air Combustion Symposium, Hsinchu, Taiwan. (1999).

[8] Yang, W. and Blasiak, W., Numerical Simulation of Properties of a LPG Flame with High Temperature Air. *International journal of Thermal Sciences*, **44** (10), p. 973(2005).

[9] Blasiak, W., Szewczyk, D. and Dobski, T., Influence of N_2 Addition on Combustion of Single Jet of Methane in Highly Preheated Air, Proc. International Joint Power Generation Conference (IJPGC2001-19048), (2001).

[10] Yang, W. and Blasiak, W., Numerical Study of Fuel Temperature Influence on Single Gas Jet Combustion in Highly Preheated and Oxygen Deficient Air. *Energy*, **30**(2-4), 385(2005).

[11] Lille, S., Blasiak, W. and Jewartowski, M., Experimental Study of the Fuel Jet Combustion in High Temperature and Low Oxygen Content Exhaust Gases, *Energy*, **30**(2-4), p. 373(2005).

[12] Mortberg, M., Study Gas Fuel Jet Burning in Low Oxygen Content and High Temperature Oxidizer, PhD Thesis, Royal Institute of Technology, Stockholm, (2005).

[13] Abbasi Khazaei, K., Advanced Furnace Modeling and Simulation, Msc Thesis, Tarbiat Modaress University, Tehran, (1995).

[14] Truelove, J S., "Heat Exchanger Design Handbook", Hemisphere Publishing Corporation, New York (1983).

[15] Launder, B E. and Spalding, D B., "Mathematical Models of Turbulence", Academic Press, New York (1972).

[16] Fluent5 Manual, Fluent Incorporation, (1998).

[17] Pun, W M. and Spalding, D B., A Procedure for Predicting the Velocity and Temperature Distributions in a Confined, Steady, Turbulent, Gaseous, Diffusion Flame, Proc. International Astronautical Federation Meeting, (1967).

[18] Khalil, E E., Spalding, D B. and Whitlaw, J H., The Calculation of Local Flow Properties in Two Dimensional Furnaces. *International Journal of Heat and Mass Transfer*, **18**, p. 775(1975).

[19] Gosman, A D., Pun, W M., Runchal A K, Spalding D B and Wolfshetein M, "Heat and Mass Transfer in Recirculating Flow", Imperial College, London (1969).

[20] Gosman, A D. and Lockwood, F C., Incorporation of Flux Model for Radiation into a Finite Difference Procedure for Furnace Calculation, Proc. 14th International Combustion Symposium, combustion Institute, p. 661(1972).

[21] Varga, R S., "Matrix iterative analysis", Prentice-Hall International, London (1962).

[22] Nogay, R. and Prasad, A., Better Design Method for Fired Heaters, *Hydrocarbon Processing*, **64**(11), p. 91(1985).

[23] Ghia, K N., Torda, T P. and Lavan, Z., Turbulent Mixing in the Initial Region of Heterogeneous Axisymmetric Coaxial Confined Jets, Report No: NASA CR-1615, Illinois Institute of Technology, Chicago (1970).

[24] Hutchinson, P. and Khalil, E E., The Calculation of Furnace Flow Properties and Their Experimental Verification, *Heat Transfer*, **98**(2), p. 276 (1976).

[25] Blasiak, W., Yang, W H. and Rafidi, N., Physical Properties of a LPG Flame with High Temperature Air on a Regenerative Burner, *Combustion and Flame*, **136**(4), p. 567(2004).

[26] Yuan, J. and Naruse, I., Effects of Air Dilution on Highly Preheated Air Combustion in a Regenerative Furnace, *Energy & Fuels*, **13**(1), p. 99 (1998).

[27] Rafidi, N., Thermodynamic Aspects and Heat Transfer Characteristics of HiTAC Furnaces with Regenerators, PhD Thesis, Royal Institute of Technology, Stockholm, (2005).

[28] Morita, M., Optimal Design for High Performance Industrial Furnace Applied High Temperature Air Combustion Technology, Proc. International Joint Power Generation Conference (IJPGC2000-15030), (2000).